# Steady State Formation of a Toroidal Electron Cloud

S. S. Khirwadkar, P. I. John, K. Avinash, A. K. Agarwal, and P. K. Kaw
*Institute For Plasma Research, Bhat, Gandhinagar 382 424, India*
(Received 24 May 1993)

A novel scheme of injection and confinement of electrons is reported for the formation of a toroidal electron cloud in the presence of a static toroidal magnetic field. The scheme is based on the use of a combination of externally applied electric field and the self-consistent space charge field for the electron trapping and confinement. The time development of electron cloud potentials measured in the poloidal plane of the torus is presented. A potential well depth exceeding the initial kinetic energy of the electrons is observed, indicating collective effects. The effect of external field on the total charge and capacitance of the electron cloud is also presented.

PACS numbers: 52.25.Wz, 52.55.Lf

The early theoretical work on drift of particles in a toroidal magnetic confinement device by Budker [1] has pointed out that either a poloidal magnetic field or an electric field along the minor radius is necessary to overcome toroidal drifts responsible for particle losses. The latter can be self-consistently generated by confining a single species plasma of appropriate charge density. Theoretical work [2] on toroidal electron clouds has shown the existence of equilibrium with closed drift surfaces under very general conditions. Furthermore, the possibility of exceeding the Brillouin limit, which may have interesting fusion reactor implications, has been shown recently [3]. Experiments with toroidal electron clouds [4–6] have proved the validity of many of the basic concepts like the existence of an equilibrium, good confinement properties, toroidal effects, etc.

The concept of electrostatic trapping of charged particles in the deep potential wells associated with a space charge cloud have led to many interesting accelerator and fusion devices. A few examples are electrostatic thermonuclear fusion reactor [7], heavy ion accelerator [8], source of highly stripped heavy ions [9], modified betatron [10], and stellatron [11]. The concept of a totally non-neutral ion torus, where high energy ions are confined by their own space charge field, may, being relatively free of transport losses of conventional neutral plasma, lead to an ideal thermonuclear reactor; however, this idea requires further quantitative examination.

In all the earlier experiments, electron injection was achieved by the so-called inductive charging process [4] based on the principle that, in the guiding center approximation, both the electrons and the magnetic flux lines in an inductor move in the direction of Poynting's vector with the common $(\mathbf{E}\times\mathbf{B})/B^2$ velocity. Thus, if a flux tube is initially loaded with electrons as it enters the inductor, a rising magnetic field would carry a current of unneutralized electrons into the device. This scheme is not suitable for the applications mentioned above because of the following fundamental limitations: (a) A monotonically increasing magnetic field is necessary for the electron injection, (b) the injection current is proportional to the rate of increase of magnetic field, (c) the time available for injection is limited by the energy available in the current source, and (d) electron losses cannot be compensated by injection of extra electrons.

An alternative, steady state injection scheme free from the above drawbacks will be of interest to practical toroidal non-neutral plasma devices. The present paper proposes such a concept and demonstrates its feasibility. The injection scheme is based on utilizing the inherent toroidal drift of charged particles to bring them into the trapping region and the subsequent modification of these drifts into closed diocotron drift trajectories by a combination of self-consistent space charge electric field and an externally applied electric field to create trapping conditions.

Consider a purely toroidal magnetic field produced by an infinite conductor carrying a current, placed along the major axis of the torus ($Z$ axis). An electron with finite $v_\perp$ introduced in such a magnetic field will start drifting along the $+Z$ direction under the influence of $\nabla\mathbf{B}\times\mathbf{B}$ drift. However, this drift will also result in a loss unless interrupted by some other mechanism. The most effective way is to apply an electric field ($\mathbf{E}r_{\text{ext}}$) in the major radial direction so that the $\mathbf{E}r_{\text{ext}}\times\mathbf{B}$ drift will oppose the $\nabla\mathbf{B}\times\mathbf{B}$ drift. This major radial electric field can be self-consistently generated by the drifting electron stream if it exceeds a critical density or can be generated by an appropriate combination of external and space charge fields such that the injected electrons will accumulate in the torus.

This concept was tried out in an experimental device, schematically shown in Fig. 1. The torus has a rectangular poloidal cross section of 28.0 cm×17.5 cm with major radius of 13.2 cm (aspect ratio of 1.5). The inner, outer, top, and bottom walls are electrically isolated from each other. The bottom wall is made of three isolated concentric circular sectors which are used as wall probes. The inner wall can be biased positively to create the major radial electric field. All other walls are grounded separately. The torus is pumped to a base pressure of $3\times10^{-7}$ torr. The toroidal magnetic field is produced by a twelve turn inductor wound symmetrically around the poloidal cross section. The electron injector is a toroidally symmetric magnetically insulated diode made up of a hot tungsten cathode and a grounded concentric cylindrical


0031-9007/93/71(26)/4334(4)$06.00

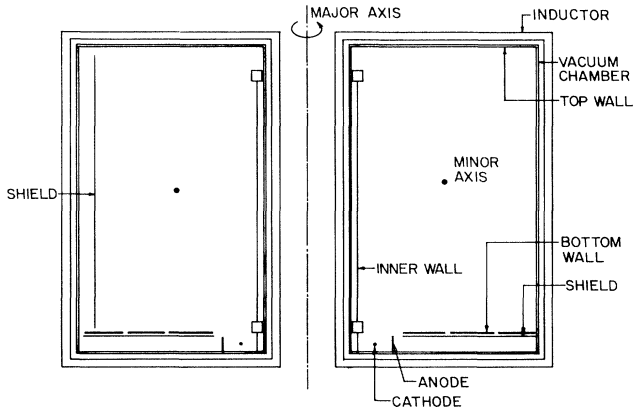


FIG. 1. Schematic diagram of the experimental device.

anode. The injector radius (7.5 cm) is less than the major radius of the torus (13.2 cm). It is placed below an annular cut in the bottom wall, allowing the emitted electrons to enter the torus. The error fields generated due to in-vacuum lead wires biasing various electrodes were seen to affect the equilibrium of the cloud and hence were shielded carefully. The injector is switched *on* at the flat top of the magnetic field. The average magnetic field at the injector is well above the Hull cutoff field [12] required for magnetic insulation.

The process of electron cloud formation is diagnosed by measuring the cloud potential with a Langmuir probe terminated across a high impedence (100 MΩ) attenuator having good frequency response. The potential measurement done with 10 times reduction in the terminating impedence (10 MΩ) resulted in only a 1% decrease in measured cloud potential, verifying the fact that current drawn by the probe is small and does not perturb the electron cloud. The potential measurements are reproducible within 2% error.

Electron current is measured at various boundaries to obtain wall losses. In the absence of any external electrostatic fields, the top wall starts collecting electron current after a time delay of nearly 10 μsec and collects nearly 60% of the total cathode emission current ($Ie_{\text{total}} = 10$ mA) continuously. The rest of the 40% electrons can be accounted for if losses at the other walls are taken into consideration. The current collected at the inner wall and the bottom wall together is found to be only 5% of $Ie_{\text{total}}$, which implies that a considerable (35%) electron loss is occurring at the outer wall. The effective reduction in the vertical drift motion of electrons due to the applied major-radial electric field is verified by observing the time delay in the collection of electrons and the average current collected at the top wall for different positive biases on the inner wall. The increase of inner wall bias from 0 to +150 V resulted in the increase of time delay by 78% (from 9 μsec to 16 μsec) and a decrease in average current collected at the top wall by 29% (from 7 mA to 5 mA).

Temporal evolution of the equipotential contours on time scales long compared to the diocotron period with a steady bias of +300 V on the inner wall is shown in Fig. 2. The initial cloud formation process starts near the injector at a major radius close to the injector radius as can be seen from Fig. 2(a). The equipotentials expand with time in both the major and minor radii, indicating continuous electron accumulation. Figure 3(a) shows the time evolution of potential contours measured at various radial locations [$\Phi = \Phi(R, t)$] in the midplane. These potential contours indicate substantial modification of the applied vacuum fields by the effect of the self-consistent field of the electrons. The electron cloud evolves with a single hump in the potential profile and the peak potential exceeds the cathode potential of 280 V.

The drifting electron stream can generate an electric field along the major radius due to induction of image charges on the wall even when the inner wall is not biased. Cloud nucleation could be started self-consistently by this image electric field and it was observed that the

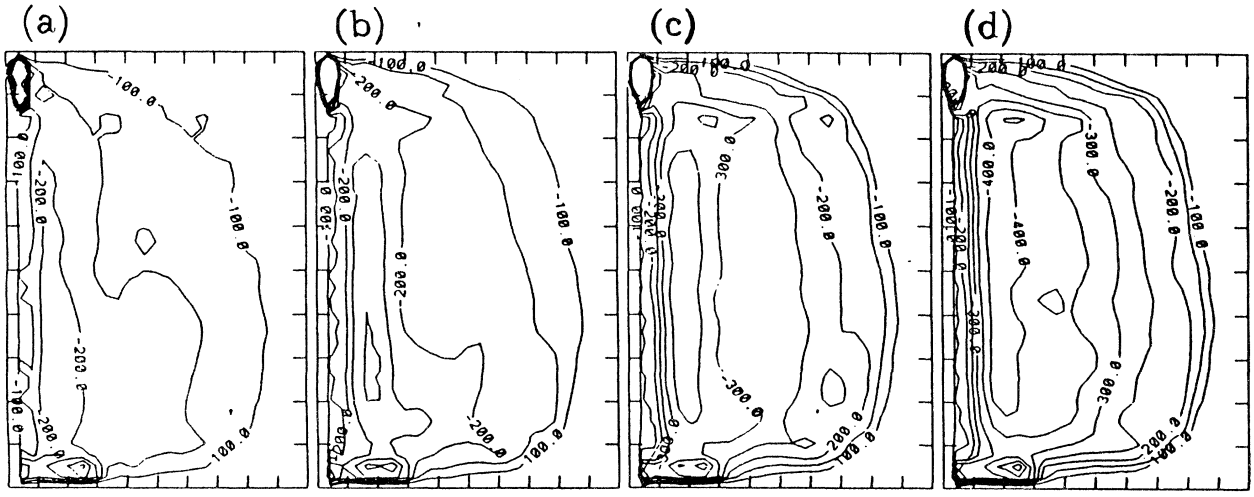


FIG. 2. Equipotential contours at (a) 50 μsec, (b) 100 μsec, (c) 250 μsec, and (d) 500 μsec.

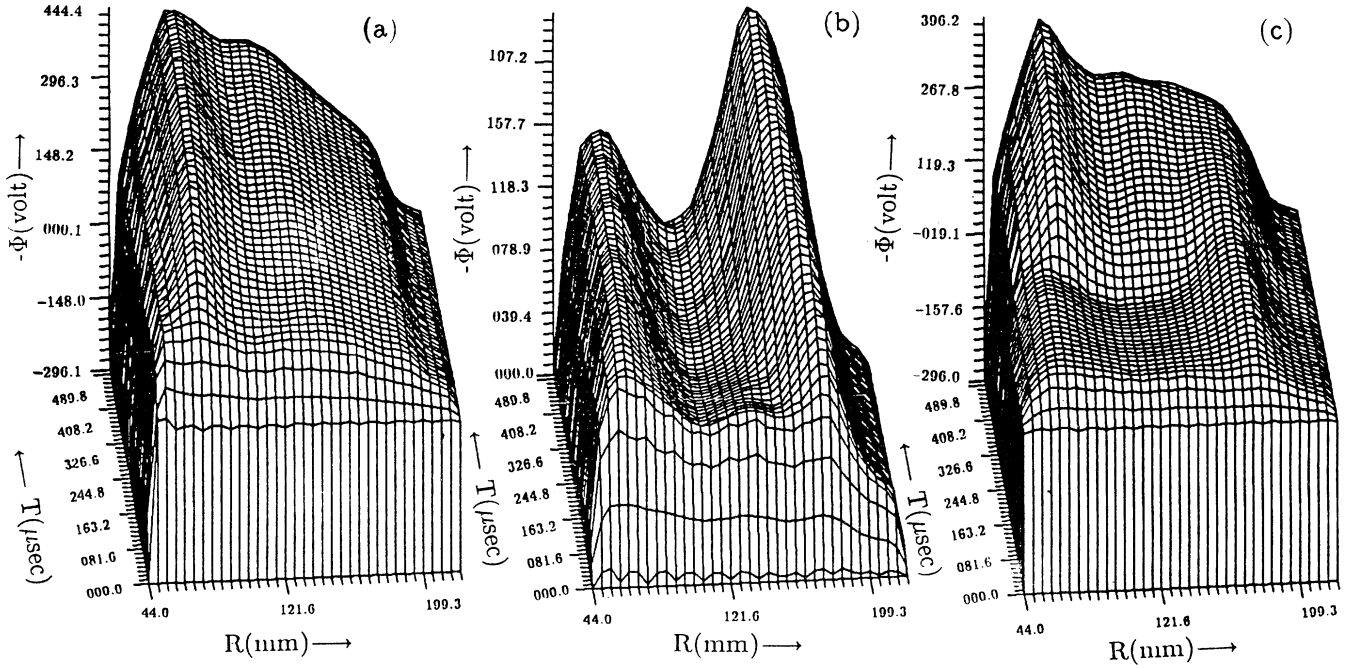


FIG. 3. Temporal evolution of cloud potentials at the midplane of the torus for inner wall biased to (a) +300 V from $t = 0$ to 500 $\mu$sec, (b) 0 V from $t = 0$ to 500 $\mu$sec, and (c) 0 V from $t = 0$ to 250 $\mu$sec and +300 V from $t = 250$ to 500 $\mu$sec.

potential well does form in this case if the emission current is above 6 mA, implying a critical density for generating an effective radial electric field. However, the potential well formed in this manner is found to be hollow as shown in Fig. 3(b). The hollow profile could be due to trapping of positive ions formed due to ionization of the background neutrals. The density profiles generated by the numerical integration of the potential profiles indeed support this [see Figs. 4(a) and 4(b)].

The role of the external electrostatic field in improving the electron confinement is verified by altering the positive bias applied on the inner wall. For the inner wall potentials above a certain critical value the potential profile retained the single hump nature and the magnitude of peak potential was found to increase with the inner wall bias.

The asymmetry of potential profile formed with the inner wall bias provides a natural mechanism for purging of the ions created by the ionization of the background gas. To verify this, we performed an experiment in which the cloud was allowed to be formed initially with the unbiased inner wall. After 250 $\mu$sec, by which time a hollow profile was formed, the inner wall bias was turned on. The recovery of the hollow profile to a solid profile is clearly seen in Fig. 3(c). The electron density without and with external field is shown in Figs. 4(b) and 4(c), respectively.

The numerical computation of total charge ($Q$) and the capacitance $C$ from the experimentally measured potential data shows some interesting collective effects and interaction of the external electric field with the electron cloud. The application of external field resulted in a net increase of $Q$ from $-14.7\times10^{-9}$ C to $-19.4\times10^{-9}$ C [see Fig. 5(a)]. (The decrease in $Q$ with time after 360 $\mu$sec can be due to the continuous ionization of the neutrals.) The capacitance of the electron cloud is calculated during the transient phase when $Q$ is increasing with time. The capacitance $C$ is given by

$$\frac{\epsilon_0}{2}\int V\overline{E}\,\overline{dS} + \frac{\epsilon_0}{2}\int E^2\,d\tau = \frac{Q^2}{2C},$$

where the left side is the total electrostatic energy ($W$) inside the surface $S$ confining the total charge $Q$. Figure 5(b) shows the plot of $Q^2$ vs $2W$ where it can be seen that the capacitance of the electron cloud $C = Q^2/2W$ changes during the transient phase. In fact, with the application of external field, the increase in $Q^2$ is slow as compared to the increase in $W$, which results in a decrease of the capacitance of electron cloud. This nonlinear nature of the $Q$-$C$ relationship, which implies collective effects, may have interesting device applications.

The dynamic equilibrium between electrons lost from the cloud and the electrons injected for their compensation could be inferred from the observation that electron cloud potentials develop as long as the injector is *on*. However, after switching *off* the injector, the cloud potential starts decaying with a typical $e$-folding time of 270 $\mu$sec. The bottom wall probes have shown the presence of oscillations which were confirmed to be due to ionization of the background neutrals because of its dependence on the background pressure. These oscillations, which were found to be suppressed as long as the external radial electric field is applied, reappeared after removal of it [13].

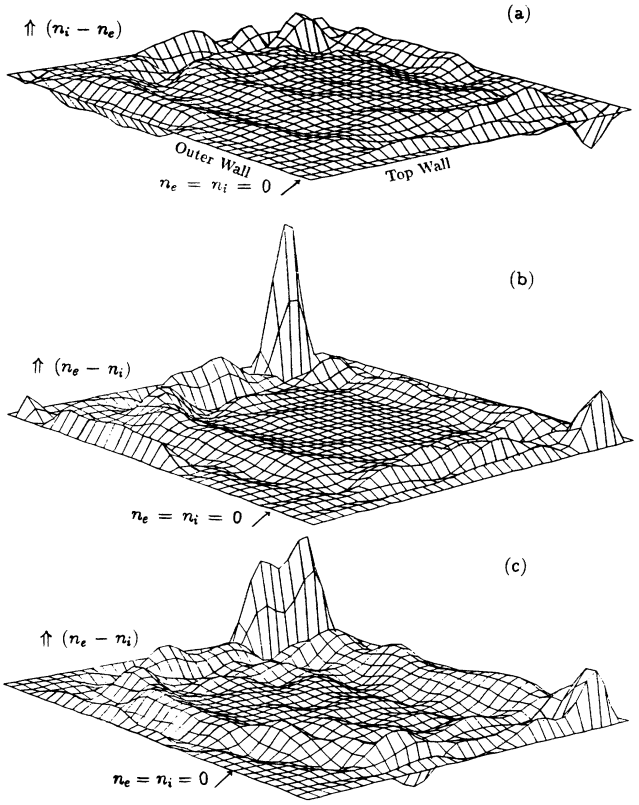


FIG. 4. (a) Ion density profile at $t = 240$ $\mu$sec. Electron density profile at (b) $t = 240$ $\mu$sec and (c) $t = 500$ $\mu$sec. The inner wall bias is changed from 0 to +300 V at $t = 250$ $\mu$sec.

This also confirms the fact that ions are purged by the application of the inner wall bias.

The observation of peak cloud potentials exceeding the injector potential suggests particle transport due to collective processes. These are time averaged potentials and cannot be ascribed to transient potential buildup over plasma or cyclotron time scales [14]. The interaction of the rotating confined cloud with the stream of unconfined electrons flowing from the injector to the wall along the outer surface of the cloud may lead to a diocotron instability resulting in particle transport across equipotentials and a resultant increase of the cloud potential. However, detailed theoretical analysis needs to be done to explain these observations.

To summarize, we have experimentally demonstrated the formation and maintenance of a low-density electron cloud in a toroidal device under steady state conditions. Study of the time development of cloud potentials gives a clear insight of the cloud formation process. It is shown that the external electrostatic fields can significantly improve the equilibrium and confinement properties of the toroidal electron clouds. The dependence of the capacitance on the trapped charge is a newly observed feature of electron clouds and implies collective processes. Further experiments to gain a detailed understanding of the processes like increase of electron density with external electrostatic fields, potential well depth exceeding the initial kinetic energy of the electrons, filling up of the hollow potential profile with external electric fields, the rapid electron transport resulting in poor confinement time after switching *off* the injector, oscillations due to ionization of the background neutrals, etc., are in progress.

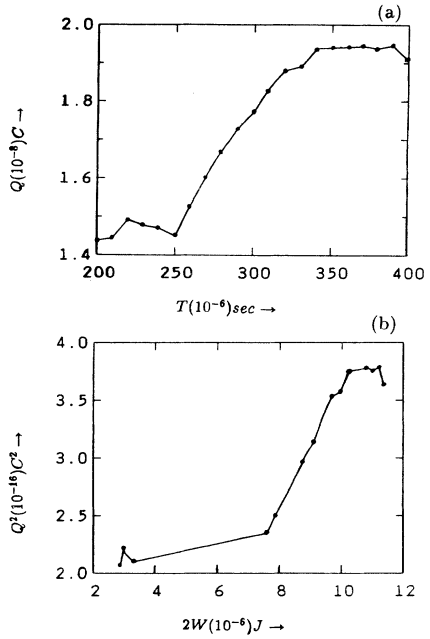


FIG. 5. (a) Total charge ($Q$) vs time ($t$); the inner wall bias is changed from 0 to +300 V at $t = 250$ $\mu$sec. (b) $Q^2$ vs 2×(total energy) ($W$).

[1] G. I. Budker, "Plasma Physics and the Problem of Controlled Thermonuclear Reactions," edited by M. A. Leontovich (Pergamon, New York, 1961), Vol. 1, p. 78.
[2] J. D. Daugherty and R. H. Levy, Phys. Fluids **10**, 155 (1967); also, S. N. Bhattacharyya and K. Avinash, Phys. Fluids B **4**, 1702 (1992).
[3] L. Turner and D. C. Barnes, Phys. Rev. Lett. **70**, 798 (1993); also, K. Avinash *et al.*, Phys. Fluids B **4**, 3863 (1992).
[4] J. D. Daugherty, J. E. Eninger, and G. S. Janes, Phys. Fluids **12**, 2677 (1969).
[5] W. Clark *et al.*, Phys. Rev. Lett. **37**, 592 (1976).
[6] P. Zaveri *et al.*, Phys. Rev. Lett. **68**, 3295 (1992).
[7] W. Clark *et al.*, in Proceedings of the Sixth Symposium on Engineering Problems of Fusion Research, San Diego, 1975 (unpublished); also, T. H. Stix, Phys. Rev. Lett. **24**, 135 (1970).
[8] G. S. Janes *et al.*, Phys. Rev. **145**, 925 (1966).
[9] J. D. Daugherty *et al.*, Phys. Rev. Lett. **20**, 369 (1968).
[10] H. Ishizuka *et al.*, Phys. Rev. Lett. **53**, 266 (1984).
[11] A. V. Deniz, J. Appl. Phys. **69**, 1151 (1991).
[12] W. A. Hull, Phys. Rev. **18**, 13 (1921).
[13] P. I. John, Plasma Phys. Controlled Fusion **34**, 2053 (1992).
[14] D. C. Barnes and L. Turner, Phys. Fluids B **4**, 3890 (1992).